E316-15 electrodes. Welded components are often subjected to heat treatment at various stages of manufacturing cycle for providing dimensional stability, stress relieving and for restoring desired mechanical properties and corrosion resistance. Due to higher carbon content of indigenously developed welding electrode, critical cooling rates for avoiding sensitization of the welded components after solution annealing is higher than that of the base metal. It has been established earlier that a cooling rate of 65 K/h resulted in sensitization while cooling with a higher rate of 75 K/h did not cause sensitization. Slow cooling from solution annealing temperature is preferred to reduce reintroduction of residual stresses and distortion. Laser surface resolidification with modulated laser power generated a microstructure that was resistant to sensitization even when cooled at the rate of 65 K/h.

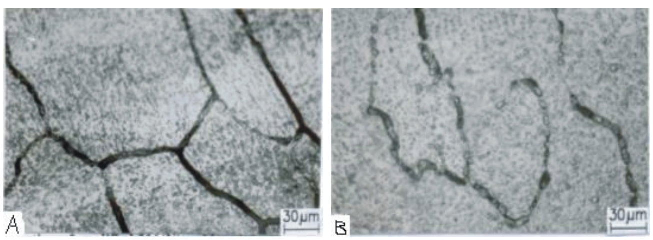

Fig. L.5.1 *Microstructures of 316 (N) weld metal after solution annealing treatment (A). Untreated base metal and (B) Laser Treated Zone.*

Laser surface treatment of modified type 316(N) weld metal were carried out with a high power CO_2 laser in CW and pulsed modes as well as with a 150 W average power pulsed Nd-YAG laser. Laser treatment conditions had a profound effect on the integrity and sensitization resistance of the treated specimen after a solution annealing treatment involving cooling at the rate of 65 K/h. Surface treated specimens with pulsed Nd-YAG laser with high peak power density and low repetition rate (3 Hz) produced numerous solidification cracks. On the other hand, surface melting with CW laser eliminated cracking but the specimens failed in intergranular corrosion (IGC) tests. However, specimens, treated with pulsed CO_2 laser at higher repetition rate (100-200 Hz) and 50% duty cycle superimposed on CW laser power (2.4kW pulses ridded over ~800W CW), not only avoided solidification cracking but also passed IGC test. In contrast to continuous grain boundary network of chromium carbide in solution-annealed base metal, fig.L.5 (A), laser surface treated region exhibited frequent discontinuities in the grain boundary network of chromium carbides, fig.L.5 (B).

(Contributed by: A K Nath, aknath@cat.ernet.in)

L.6 Improved cut quality in titanium with modulated CO_2 laser beam

Titanium finds extensive use in aerospace, medical and vacuum applications. Cutting of Titanium sheets is one of the primary requirements in the fabrication of most of the components. Non-contact laser cutting, because of its low heat input characteristics, has the capability to cut with narrow kerf width; straight cut edges, low roughness, and minimum heat affected zone (HAZ). However, initial piercing required for initiating laser cutting within the sheet and ejection of viscous molten metal for dross-free cutting usually pose problem.

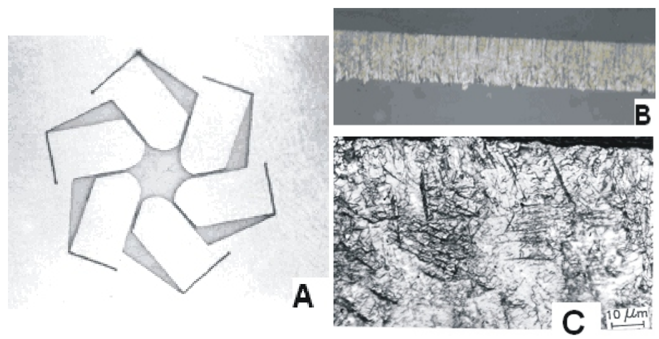

Fig. L.6.1 *A) Profile-cut Titanium sheet, B) Dross-free cut surface and C) No noticeable HAZ below cut edge. (Peak power = 600 W; frequency = 500 Hz; duty cycle = 30%, speed = 60 mm/min).*

With extensive experimental study of the dynamic behavior of melt ejection in the 1 mm thick Titanium sheet using a 3.5 kW CO_2 laser operated in continuous wave (CW) and pulsed modes and different gases e.g. Ar, He and N_2 for melt ejection, optimum laser and process parameters were established for piercing holes and dross-free profile cutting. Laser pierced holes with optimum combination of low tapering and narrow heat affected zone were created with modulated laser beam operated at high duty cycles (~80%) and Ar as shear gas for melt ejection. Dross-free cuts with no noticeable HAZ were obtained with high frequency modulated laser beam (~500 Hz) with low duty cycle (≤50%). Microscopic features of laser cut surfaces reflected the dynamic mechanism involved in laser cutting process.

(Contributed by : A K Nath, aknath@cat.ernet.in)

L.7 Characterization of magneto-optic trap

A Magneto-Optic Trap (MOT) developed for cooling and trapping of Rb atoms is shown in Fig. L.7.1. It essentially consists of a glass chamber, fabricated at the CAT Glass Blowing Facility, having eight arms sealed with optically polished windows. The chamber is pumped down to a pressure of ~ 10^{-8} mbar using a turbo molecular pump (from Vacuum Technology Lab) and a sputter-ion pump (from PD & PPD). After evacuation, Rb vapor with a pressure of ~10^{-8} mbar is produced in the chamber by passing a dc current of ~3.5 A through two Rb-getters fixed in a glass bulb fused to the chamber. A pair of coils (diameter 8 cm, number of turns 80, separation 4 cm) placed symmetrically around the glass chamber, carry equal and opposite currents to produce the magnetic field required for MOT operation. The field is zero at the centre and increases linearly with distance in the central region with a radial field gradient ~ 0.7 times the axial field gradient. The latter can be varied over a range of 5-20 G/cm by varying the coil current. All stray magnetic fields are removed by the use of three orthogonal pairs of large compensating coils. Three orthogonal pairs of σ^+ and σ^- polarized laser beams with nearly equal intensity are obtained from a frequency stabilized single-mode semiconductor diode laser (780 nm). These laser beams, which cause cooling and trapping of the atoms are aligned so as to intersect at the centre of the glass chamber. The laser beams are nearly Gaussian with a $1/e^2$ diameter of ~6 mm. Trapped cold atoms are imaged and observed using a CCD camera. H. S. Vora of LSED, has developed the CCD image grabbing and analysis software.

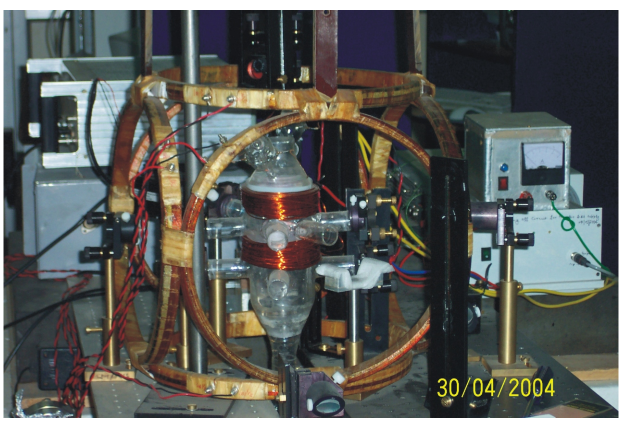

Fig. L.7.1 *Magneto-Optic Trap setup for Rb atoms.*

The MOT was recently characterized by measuring the temperature and the number of cold ^{87}Rb atoms as a function of various parameters. For these experiments, the trapping laser beams were red-detuned with respect to the cyclic transition $5^2S_{1/2}$ (F = 2) $\rightarrow$ $5^2P_{3/2}$ (F'= 3) at 780 nm, with detuning Δ_L ranging from one to four times the natural line width (FWHM) $\Gamma = 2\pi \times 5.9$ MHz. To collect sufficient number of atoms, the intensity of these beams was kept nearly three times the saturation intensity I_s (~ 1.6 mW/cm^2). To prevent optical pumping into the lower ground-state hyperfine level, 1 mW repumping laser beam - frequency locked to the peak of the $5^2S_{1/2}$ (F = 1) $\rightarrow$ $5^2P_{3/2}$ (F'= 1) transition - obtained from another similar diode laser was combined with the cooling and trapping laser beam. We estimated the number of trapped atoms in the MOT by measuring the intensity of fluorescence from the trapped atoms using a calibrated photodiode. The size of the cold atom cloud was measured using a calibrated CCD camera. The number and peak density of cold atoms were found to be around 5×10^6 and 1×10^{10} cm^{-3} respectively for an optimized laser detuning of $\Delta_L = -2\,\Gamma$ and an axial magnetic field gradient (dB/dz) of ~13 G/cm. The 'free-expansion' method was used to measure the temperature of the trapped atoms. In this method, the cold atom cloud is released from the trap and expansion rate is measured to estimate the initial temperature of the cloud. To perform these measurements, the laser beams and the magnetic field were switched off and the atom clouds undergoing free expansion was illuminated by a probe laser pulse after a variable delay.

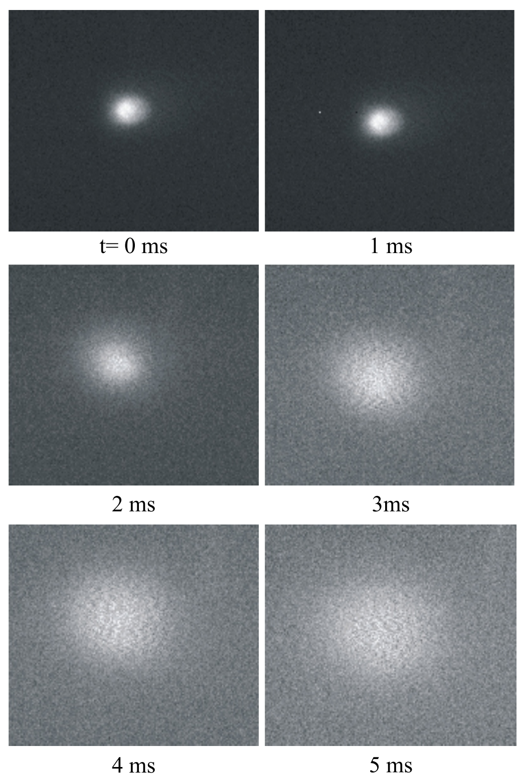

Fig. L.7.2 *Images of cold atom clouds grabbed during its free expansion .*

The fluorescence from the atoms excited by this probe pulse was used to take images of the expanding cloud. The Laser Instrumentation Section has developed the computer control for this experiment. The lowest temperature of the atom cloud was ~ 120 μK for a laser detuning Δ_L = -3.5Γ and an axial field gradient of ~13 G/cm. Fig. L.7.2 shows the images of the atom cloud at intervals of 1 ms during free expansion.

(Contributed by: S. C. Mehendale, scm@cat.ernet.in)

L.8 Highly efficient diode-side-pumped CW Nd:YAG laser

We have developed a highly efficient Diode-pumped CW Nd:YAG laser generating 195W of output power in multimode operation for the diode pump power of 423W. This corresponds to an optical-to-optical efficiency of 46% and the electrical-to-optical efficiency of 23%. This is to the best of our knowledge, the highest electrical-to-optical efficiency reported for a CW diode side-pumped Nd:YAG laser. The system consists of a Nd:YAG rod, a gold-coated flow tube and three diode pump modules. The Nd:YAG rod is 4mm in diameter and 0.9 at.% Nd-doped with finely ground barrel surface. The rod is surrounded by a gold-coated, 10mm outer diameter flow tube for water-cooling. Each diode pump module consists of three 50W water-cooled 1-cm diode laser bars (Model JOLD50-CANC-1L). The diode laser radiation is polarized >95% parallel to the fast axis.

The flow tube has gold coating on the outside surface with three narrow windows of 1.5mm width, over its length. Diode pump modules are located 0.5mm in front of the center of 3-fold symmetric windows to couple the diode beams into the flow tube. The temperature of water for cooling the diode bar is set to 19.5°C, where the center wavelength of the diode modules is about 805.4nm at maximum driving current. Although the center wavelength deviates from the absorption peak of the Nd:YAG laser medium (808.5nm), the output power is maximum due to wing-pumping method. In this method peak diode emission wavelength is set near the edges of the peak absorption line of Nd:YAG to take advantage of better pumping uniformity over the cross-section of the laser rod.

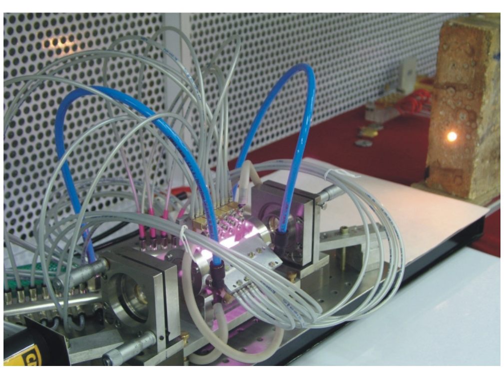

Fig. L.8.1

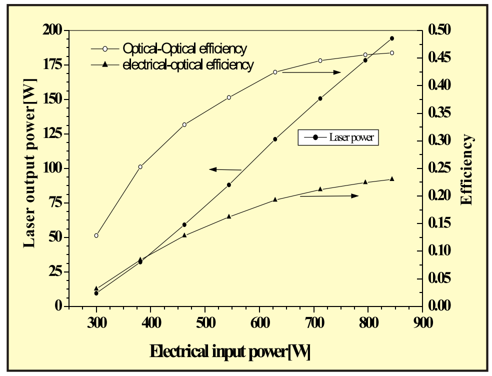

Fig. L.8.2

The output performance of the side-pumped Nd:YAG laser is investigated in multimode operation using plano-concave symmetric resonator with 5m ROC mirror with 12% transmission as output coupler. The cavity mirrors are separated at a distance of 125mm. Figure L.8.1 & L.8.2 show the system photo and characteristics of the output power and efficiencies versus input electrical pump power. The pumping efficiency has been measured by pump power leakage analysis method and it is found to be more than 94%. The pumping efficiency is defined as the ratio of the power absorbed by the rod to the total diode pump power. The high efficiency of the system can be attributed to wing-pumping method resulting in uniform pump light distribution and better pumping efficiency due to p-polarized pump beams.

(Contributed by : T.P.S. Nathan; nathan@cat.ernet.in)

L.9 Compact efficient intracavity frequency doubled Nd:YAG laser producing 30W average green power

High average power green beam at 532 nm are useful for many basic research studies, industrial and medical applications. Such sources can be realized by intracavity frequency doubling in a Q-switched Nd:YAG laser. We have developed a compact linear cavity for intracavity green generation as shown in Fig.L.9.1. The cavity was a plane-plane resonator stabilized by the thermal lensing effect. The rear mirror (M1) is highly reflecting at the fundamental wavelength. The flat end mirror (M2) is highly reflecting at the fundamental wavelength and highly transmitting at the second harmonic wavelength at 532 nm. The mirror M2 was coated directly on the KTP surface. The other surface of the KTP crystal (M3) was coated highly reflecting at the second harmonic wavelength and highly transmitting at the fundamental wavelength in order to retro reflect the green beam that generated in the backward direction. The reason for coating mirrors on the KTP crystal was to minimize the